

Advances in technical aspects of myocardial perfusion SPECT imaging

Piotr J. Slomka, PhD,^a James A. Patton, PhD,^b Daniel S. Berman, MD,^a and Guido Germano, PhD^a

Although myocardial perfusion SPECT (MPS) imaging is widely used in current clinical practice, it suffers from some fundamental limitations including long image acquisition, low image resolution, and patient radiation dose. In the last two decades, MPS was performed most commonly by standard dual-head scintillation cameras with parallel-hole collimators, typically configured in a 90° detector geometry and image reconstruction based on standard filtered-back projection algorithms. The required scan times were as long as 15-20 minutes for each stress and rest MPS acquisition to provide adequate imaging statistics, resulting in long overall test times and frequent artifacts caused by patient motion during the scan as well as compromised patient comfort. Recently, it has become very important to address these limitations, since MPS has new competitors in the non-invasive imaging arena most notably coronary CT angiography (CCTA), which allow diagnostic imaging in a very short time. In addition, a practice of combining MPS with other modalities such as CCTA for better diagnostic certainty¹ has intensified concerns regarding total radiation dose delivered to the patient.² The radiation dose and acquisition time are intrinsically linked with each other, as longer acquisition times could be used with lower injected doses and higher doses could be used to shorten acquisition times.

There have been significant recent efforts by industry and academia to develop new imaging systems with increased sensitivity and new methods of image reconstruction optimizing image quality, which will simultaneously allow higher photon sensitivity and improve both image quality and resolution. These efforts

address the main limitations of MPS by combining several approaches such as changing the detector geometry and optimizing tomographic sampling of the field of view for myocardial imaging, improving the detector material and collimator design, and optimizing the image reconstruction algorithms. In this review article we summarize these developments.

NEW HARDWARE FOR OPTIMIZED MPS IMAGING

Several new dedicated hardware camera systems with optimized acquisition geometry, collimator design, and associated reconstruction software have been recently introduced by various vendors. Innovative designs of the gantry and detectors have been proposed which allow increased sampling of the myocardial region, and thus allow better local sensitivity. These systems combine an improvement in spatial resolution and sensitivity. By faster imaging times due to increased sensitivity and by eliminating the need to position the patient's arms above the head by imaging in an upright or reclining position, patient comfort is dramatically improved. As a consequence of faster imaging times and more comfortable patient positioning, these systems have the additional benefit of reducing patient motion during a scan. Furthermore, claustrophobic effects are reduced and the floor space requirements are more flexible since the new detectors and the associated mechanical are significantly smaller in comparison to standard equipment.

DIGIRAD CARDIUS 3 XPO

Digirad, Inc. (Poway, CA) has developed a Cardius XPO camera dedicated to fast cardiac imaging. This system can be configured in 2- or 3-detector configurations.³ The Cardius 3 camera and its geometry (triple-head configuration) is shown in Figure 1. These models use indirect, solid-state detectors consisting of pixilated CsI(Tl) and photodiodes to configure detector heads that are more compact than conventional cameras, equipped with photomultipliers. Each detector head is 21.2 × 15.8 cm and contains an array of 768 6.1 × 6.1 × 6 mm thick CsI(Tl) crystals, coupled to individual silicon photodiodes, which are used to convert the light

From the Departments of Imaging and Medicine,^a AIM Program, Cedars-Sinai Medical Center, Los Angeles, CA; Department of Radiology and Radiological Sciences,^b Vanderbilt University Medical Center, Nashville, TN.

Received for publication Dec 30, 2008; final revision accepted Jan 6, 2009.

Reprint requests: Piotr J. Slomka, PhD, Departments of Imaging and Medicine, AIM Program, Cedars-Sinai Medical Center, Los Angeles, CA, USA; slomkap@cshs.org.

J Nucl Cardiol 2009;16:255-76.

1071-3581/\$34.00

Copyright © 2009 by the American Society of Nuclear Cardiology.

doi:10.1007/s12350-009-9052-6

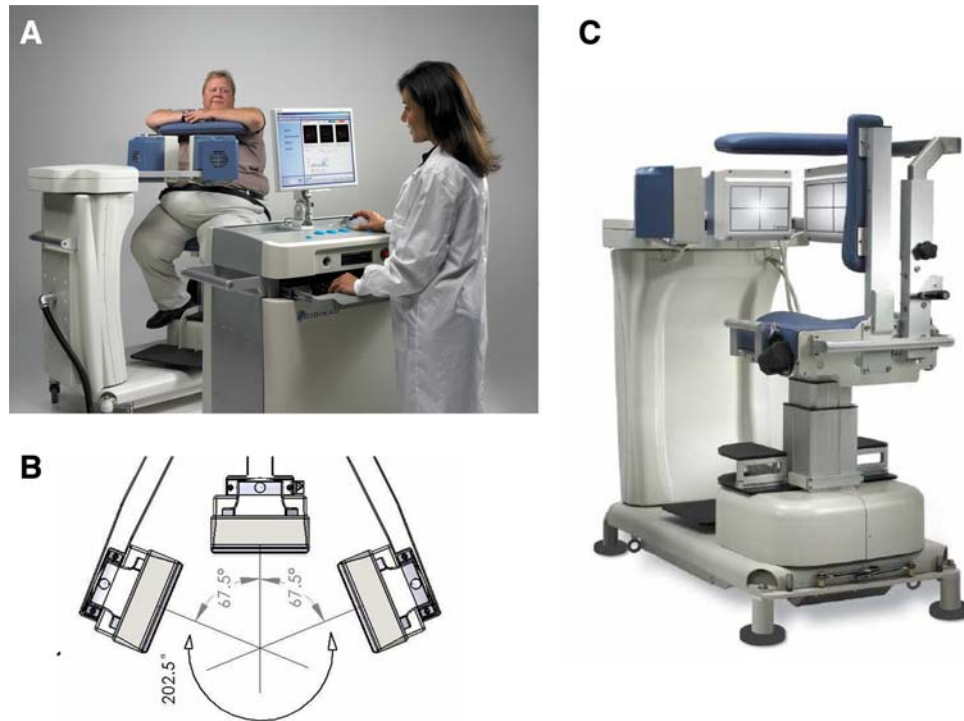


Figure 1. Upright patient position on the Digirad Cardius 3 XPO (C 3 XPO) triple-head, pixilated detector camera (A), its geometry (B), and a photograph of the camera (C). Detectors remain fixed while patient is rotated through 202.5° in a rotating chair. Images courtesy of Digirad, San Diego, CA.

output of the crystals to electrical pulses. Digital logic and software is used to process the signals and create images instead of analog Anger positioning circuits. In the 3-detector system the detector heads are positioned at 67.5° between heads, as shown in Figure 1B. Heads are allowed to be moved in and out (closer to or farther away from the patient). For imaging, the patient sits on a chair with his arms placed on an arm rest above the detectors. Data acquisition is typically accomplished in 7.5 minutes by rotating the patient chair by 67.5°, producing a total acquisition arc of 202.5°. With this system the manufacturer reports a reconstructed spatial resolution of 8.95 mm (at a 20 cm orbit radius) and a sensitivity of 234 cpm/ μ Ci, using the system's cardiac collimator and a 3D version of the ordered subsets expectation maximization (OSEM) approach for reconstruction. These systems are now used clinically in several sites, and reports have been published comparing their performance to that of a standard dual-headed camera when it was found that the similar quality could be obtained with 38% reduction in the acquisition time.⁴

Data have recently shown that the acquisition time can be further reduced with this scanner by the application of optimized image reconstruction protocols,

developed by Digirad. The nSPEED reconstruction⁵ models the depth-dependent detector spatial response of the SPECT systems with a 3D version of the OSEM reconstruction method. In the preliminary results from the multi-center trial (10 sites) with 448 patients, the image quality improvement with nSPEED was compared to a conventional 2D-OSEM technique.⁶ The trial demonstrated that nSPEED applied to data obtained with Cardius-3 camera enables the reduction of the acquisition time by 50%, while maintaining image quality and information with diagnostically equivalent images for rest and stress studies as well as reliable quantification of function and perfusion. The mean imaging times were 4.2 minutes for stress and 4.8 minutes for rest with the optimized 3D reconstruction. A representative image from this trial is shown in Figure 2.

CARDIARC

CardiArc (Canton, MI) has developed a dedicated nuclear cardiology SPECT camera in which the detector and collimation are redesigned and optimized specifically for cardiac imaging.⁷ This device has no visibly moving parts and has a single internally moving part which is hidden from the patient.⁸ Therefore from the

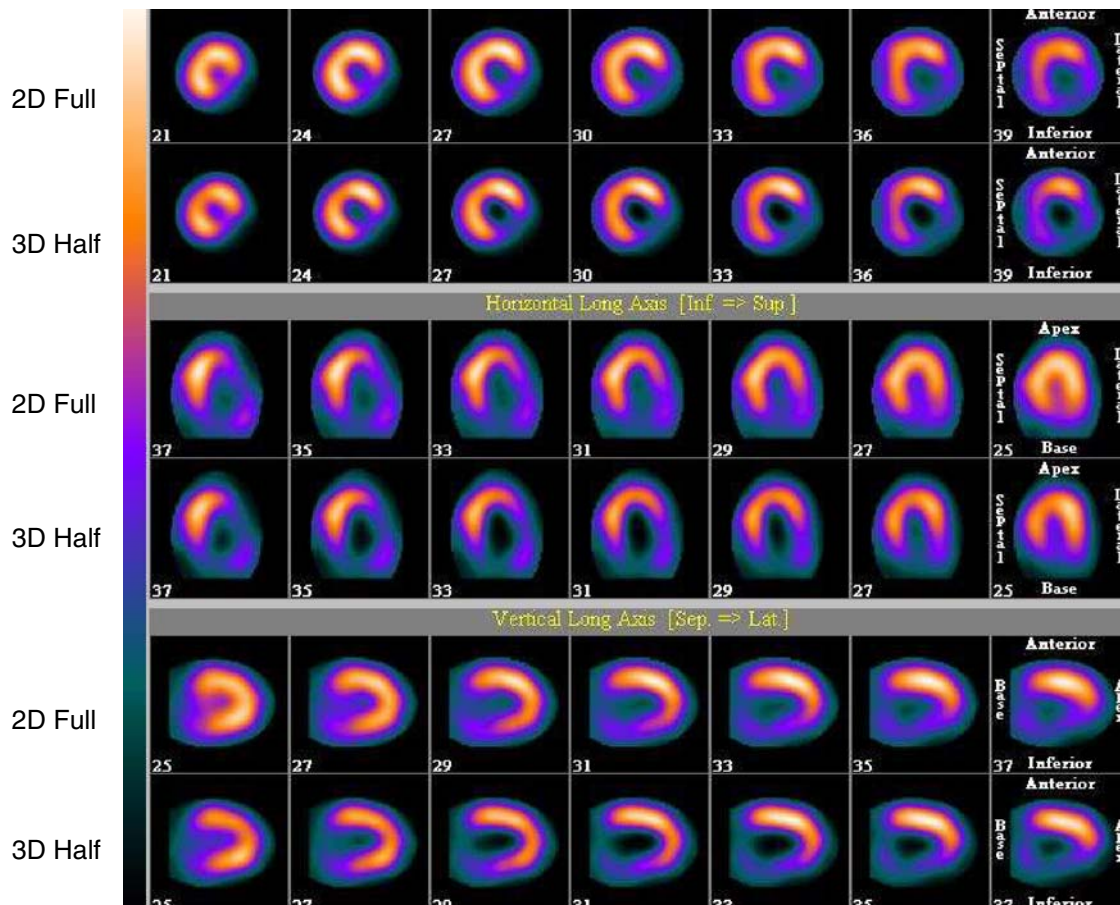


Figure 2. Images at full-time stress (6.7 minutes) and half-time (3.3 minutes) obtained with Cardius 3 XPO and n-speed reconstruction in Tc-99m sestamibi study of a male patient age: 55, stress type: exercise, height: 5'9" and weight: 183 lbs. The full-time acquisition times were 6.7 minutes for stress (20 seconds/proj) with 31 mCi Tc-99m sestamibi dose. Images courtesy of Dr. Jashmid Maddahi and Digirad, San Diego, CA⁶.

outside the detector appears motionless, and for comfort the patient is positioned upright. Scan times reported by the company are as short as 2 minutes.⁷ The camera system and a typical patient position are shown in Figure 3. This system was originally designed to use arrays of CZT crystals as detectors. However, due to high cost of CZT material and potential long-term stability issues with CZT,⁹ the detector material was changed in order to enable commercial production. Figure 4 illustrates the design and the principle of operation of the current model. The system incorporates a high high-definition, high-spatial resolution detector utilizing 3 curved NaI(Tl) crystals with graduated grooving technology and an array of 60 photomultiplier tubes arranged in three rows (Figure 4A). The detector uses a proprietary digital process developed by CardiArc that replaces the conventional Anger logic. Horizontal photon collimation in each slice is accomplished by using a thin, curved, lead sheet with 6 narrow vertical slots (Aperture Arc)

(Figure 4A). Vertical collimation is accomplished using a series of stationary lead vanes that are stacked vertically between the aperture arc and the NaI(Tl) crystals. In this way, data are collected in 1-mm-thick slices using the 6 vertical apertures to collimate photons so that they are detected continuously across the detector surface with no overlap of data from different apertures. During acquisition, the aperture arc rotates to acquire data from multiple projections providing 1,280 angular samples in 0.14° increments over 180°, which is a factor of 21 greater than a conventional camera angular sampling (typically 3°). All detector pixels are active simultaneously while photons are detected from multiple angles (Figure 4B), which provides high-efficiency imaging. The movement of the aperture arc is synchronized electronically with the areas of the NaI(Tl) crystals that are imaging the photons passing through the individual slots. The aperture arc's weight of 35 lbs is much lighter than traditional moving gantries, which facilitates precise



Figure 3. Photograph of the CardiArc SPECT-HD demonstrating patient positioning for optimal cardiac imaging and the technologist in the operating position, taking advantage of the built-in radiation shielding. Images courtesy of CardiArc, Inc.

motion control. The aperture arc movement ranges ~ 9 inches in order to cover the entire cardiac field of view, and each traverse of the arc takes 10 seconds.

SPECT reconstructed spatial resolution values (full width half maximum) quoted by CardiArc range from 3.6 mm (at 82 mm source to aperture arc distance) to 7.8 mm (at 337 mm source to aperture arc distance). An independent evaluation concluded that the CardiArc system appears to gain image quality by a factor of 5-10 when compared to the conventional dual-head camera.¹⁰ A comparison of patient imaging capabilities is shown in Figure 5.

SPECTRUM DYNAMICS

Spectrum Dynamics, Haifa, Israel, has manufactured a system called D-SPECT. The design and the principle of its operation are shown in Figure 6. The patient is imaged in a semi-upright position with the left arm placed on top of the camera (Figure 6A) or in the supine position. Acquisition time as short as 2 minutes has been reported.¹¹ This system uses pixilated CZT detector arrays (Figure 6B) mounted in 9 vertical columns and placed in a 90° gantry geometry (Figure 6C). While CZT detectors are higher in cost, they have advantages of superior energy resolution (by a factor of approximately 1.7 at 140 keV) and compact size as

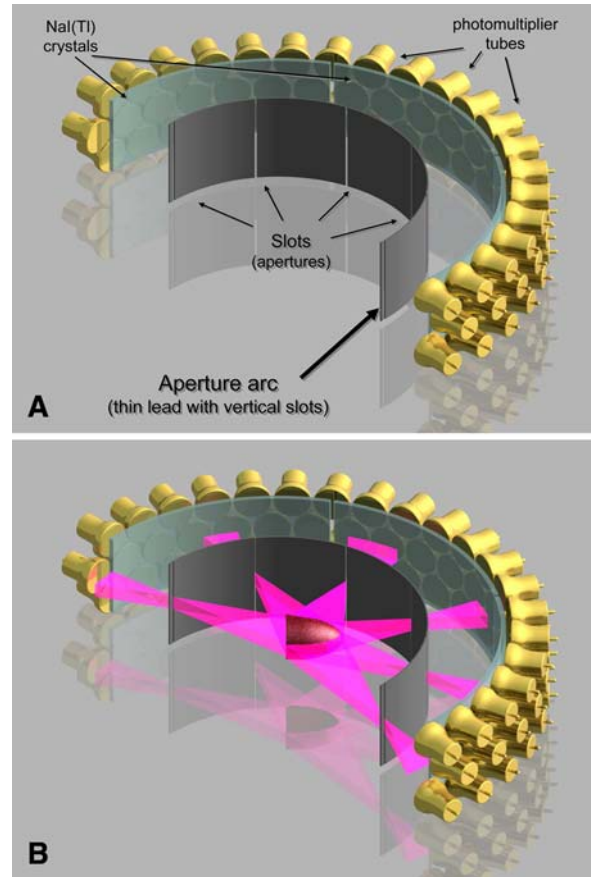


Figure 4. Design and principle of operation of CardiArc camera. The camera uses three stationary NaI(Tl) crystals and corresponding photomultiplier tubes for photon detection (A). The aperture arc has six slots (apertures) for horizontal collimation, and continuously rotates while imaging. All detector pixels are utilized simultaneously, allowing imaging multiple angles (B). Image courtesy from CardiArc, Inc., with permission.

compared to the combination of NaI(Tl) with photomultiplier tubes of the conventional Anger camera. With D-SPECT, each detector column is fixed in a mechanical mounting, and the data acquisition is performed by rotating these multiple columns in synchrony. The photons from a given location are detected at multiple angles by multiple columns as the fields of view of the detectors are swept through the region of interest. Each column (as shown in Figure 6B) consists of an array of 1024 CZT elements ($2.46 \times 2.46 \times 5$ mm thick), arranged in a 16×64 element array with an approximate size of 40×160 mm. Each column is fitted with square, parallel hole, high sensitivity collimators, such that the dimensions of each hole are matched to the size of a single detector element. The collimators are fabricated from tungsten to eliminate the production of lead x-rays that might interfere with ^{201}Tl imaging. The

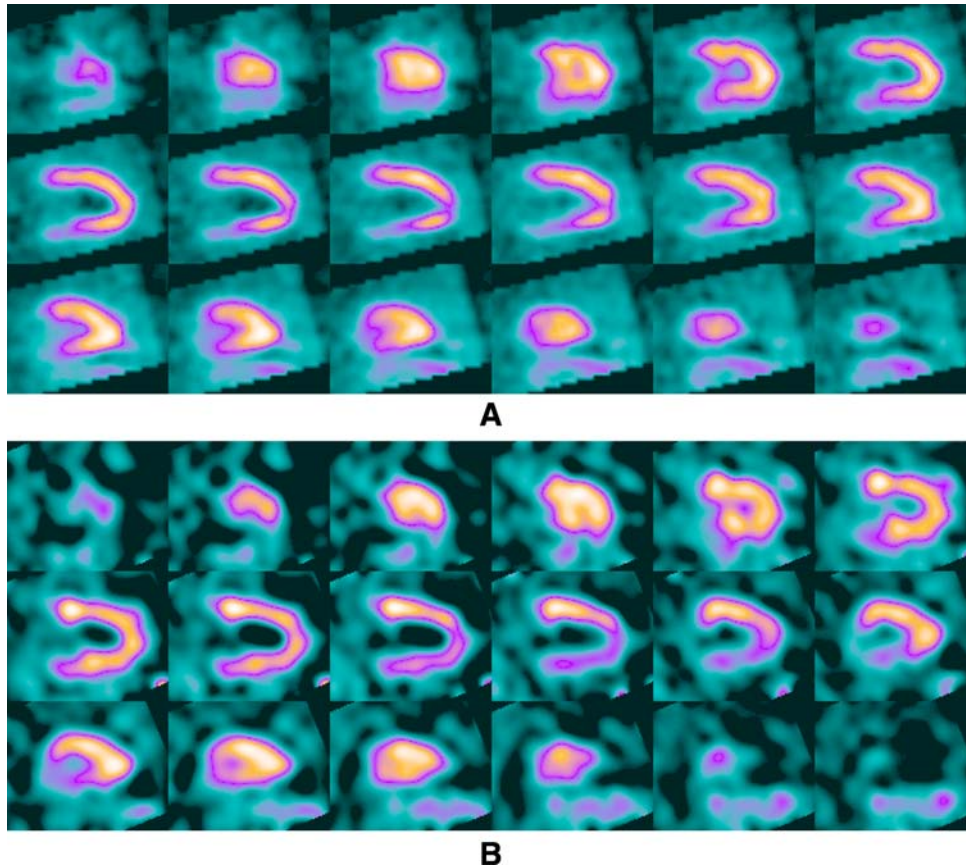


Figure 5. Stress images of a 55-year-old male, 6'5'' 235 lbs with substernal chest pain and shortness of breath. Cholesterol = 240. Developed 1.5-2.0 mm ST depression in inferior leads at stress, injected with 31.2 mCi Tc-99m sestamibi at peak stress. Image set **A**, was acquired with a conventional dual-head scintillation camera using LEHR collimators for 10.6 minutes and demonstrated an infero-basal defect. Image set **B**, was acquired with CardiArc for 4.7 minutes, and correctly demonstrated a more severe and more extensive defect in the inferior wall to the apex. Angiography revealed high-grade, proximal PDA stenosis. Image courtesy from CardiArc, Inc., with permission.

collimators have a larger effective diameter than conventional LEHR collimators used with scintillation cameras, yielding a significant gain in their geometric efficiency. The collimator has a hole length of 24.5 mm with a 2.46 mm pitch and 2.26 mm hole diameter. The compensation for the loss in geometric spatial resolution that results from this design is accomplished by the use of CZT, with its superior energy resolution, and software compensation methods. All data are collected in list mode. A proprietary Broadview™ iterative reconstruction algorithm, based on the ML-EM approach, with resolution recovery and use of the cardiac shape priors, has been developed and patented by the manufacturer.¹² The overall system resolution is 5 mm in line source experiments, superior to that of the standard Anger camera systems.

Data acquisition is accomplished in a two-step process. First, a 10-second pre-scan is performed to identify

the location of the region of interest. Scan limits and timings are then set for each detector column, and the final scan is performed with each detector column rotating within the limits set from the pre-scan data. This process is shown diagrammatically in Figure 7. This process is termed region-of-interest (ROI)-Centric scanning by the manufacturer because the scan field is limited only to the myocardial region. It is not possible to measure an absolute value of sensitivity for this system as prescribed by the NEMA quality control standards¹³ because the sensitivity is significantly dependent on the field-of-view, defined individually for each patient by the pre-scan process. However, the most centrally located point has been reported to demonstrate a sensitivity of 1407 counts/ μ Ci/minute compared to the 160-240 counts/ μ Ci/minute range generally observed with standard cameras.¹⁴ A case example showing image quality on both D-SPECT and A-SPECT, obtained with the same isotope injection, is

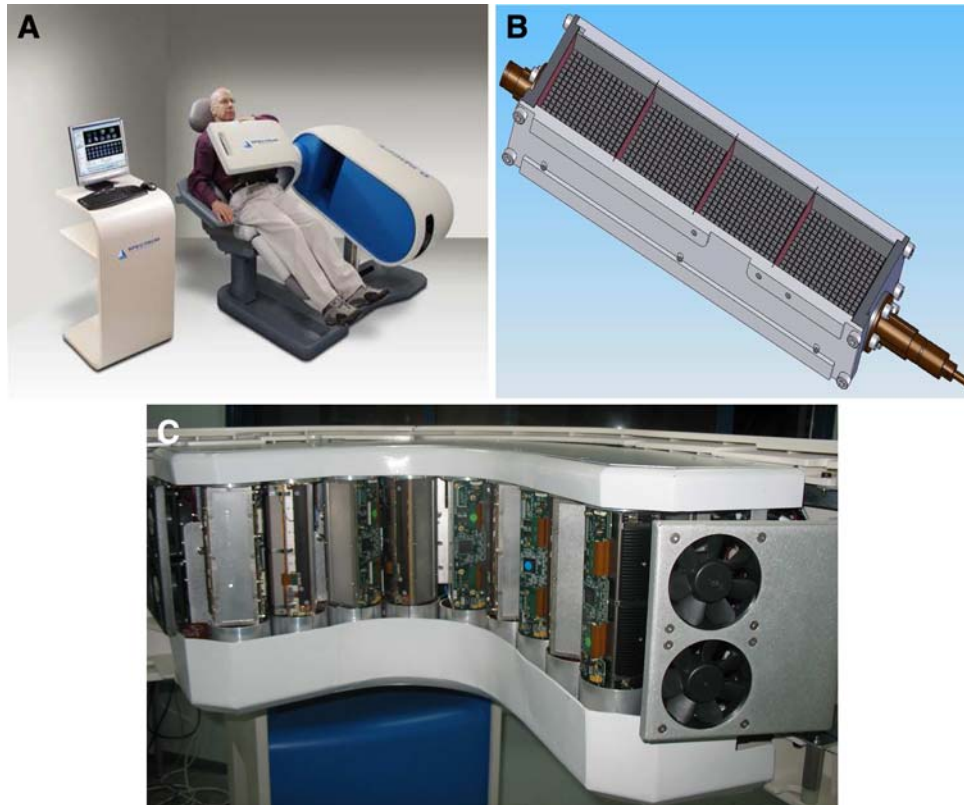


Figure 6. D-SPECT camera. Photograph of the D-SPECT camera showing patient position (A). A diagram of a single detector column from the D-SPECT camera (B), and a photograph of 9 detector columns configuration (C). Photograph courtesy of Spectrum Dynamics, Haifa, Israel.

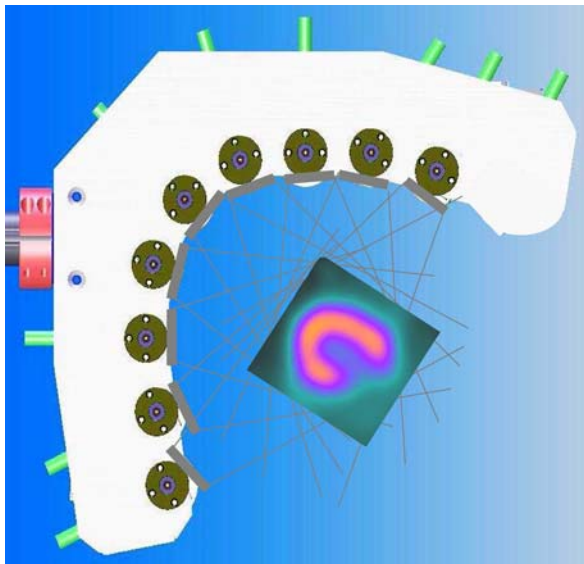


Figure 7. The ROI-centric technique utilized by the D-SPECT camera to optimize data collection from the myocardium.

shown in Figure 8. In a recently published study, when D-SPECT was compared to A-SPECT, the myocardial count rate (with the same injection of the isotope) was

7 to 8 times higher for D-SPECT (Figure 9).¹¹ Preliminary work has shown that simultaneous dual isotope SPECT MPI with this camera is feasible using Tl-201 and Tc-99m, taking advantage of the improved energy resolution of CZT.¹⁵

The higher sensitivity of this system has been exploited to develop new clinical protocols. Cedars-Sinai Medical Center has reported the routine clinical use of this scanner in over 400 patients using a stress ²⁰¹Tl (2 mCi)/rest tetrofosmin or sestamibi (8-10 mCi) protocol. Using half of the radioactivity associated with standard dual isotope procedures, this protocol includes upright and supine immediate post-stress images of 6 minutes each followed by rest injection and immediate 4-minute rest imaging. The total imaging time of this protocol is 19 minutes. Good to excellent image quality without significant extracardiac interference was observed in over 96% of the cases.¹⁶ A multi-center study conducted at Cedars-Sinai Medical Center, Miami Baptist Hospital, Vanderbilt University Medical Center and the Brigham and Women's Hospital has confirmed a close correlation and diagnostic equivalence to standard acquisition techniques using objective quantitative measures.¹⁷

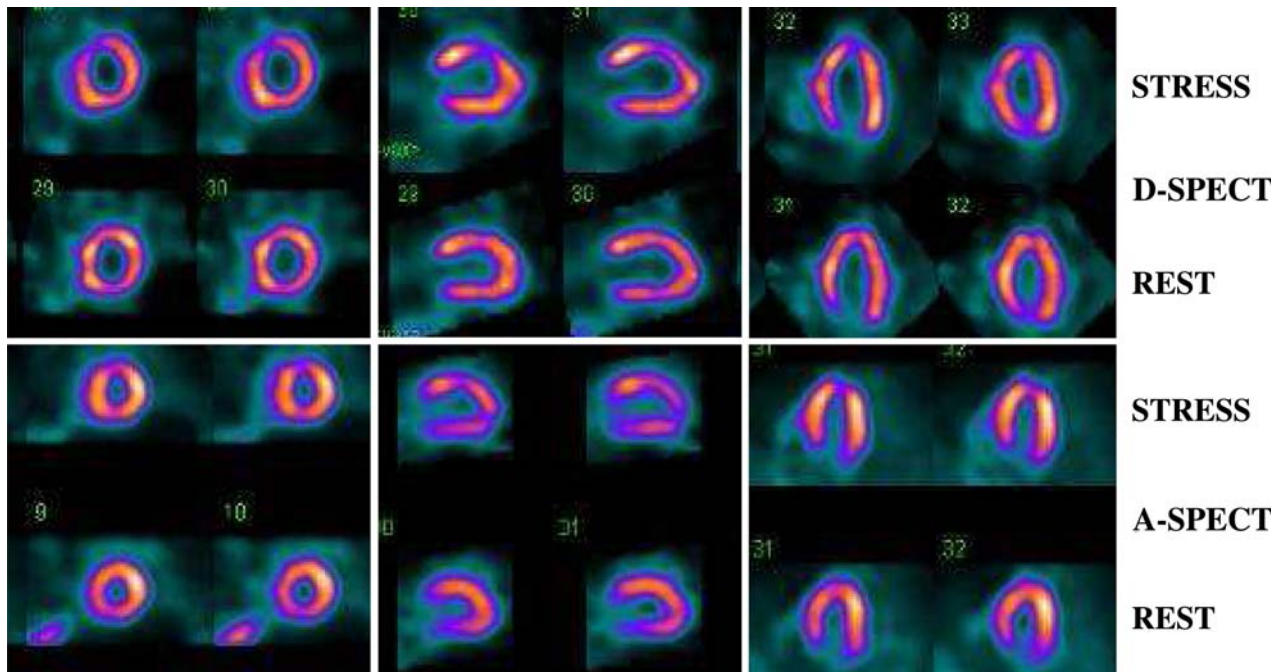


Figure 8. A study with standard dual head SPECT camera (A-SPECT) and D-SPECT. Gender: male, age: 61 years, weight: 200 lbs. Patient had history of coronary disease LAD stent, atypical angina, shortness of breath, diabetes, hypertension, or current smoking. The rest/stress MIBI protocol was performed with rest 8.2 mCi, stress 37 mCi dose. X-ray angiography found proximal to mid LAD 70% long lesion correlation. Both A-SPECT and D-SPECT correlate to coronary angiography but D-SPECT shows more ischemia correlating better to coronary angiography. The acquisition times for both stress and rest were: A-SPECT—rest 17 min, stress 15 min; D-SPECT—rest 4 min, stress 2 min. Images courtesy of Dalia Dickman (Spectrum Dynamics, Haifa, Israel).

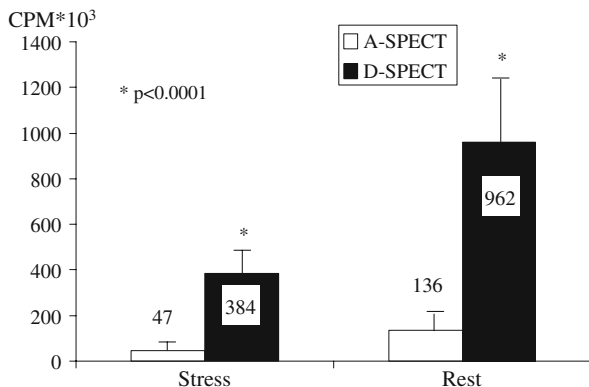


Figure 9. The higher system sensitivity of the D-SPECT system is demonstrated by a significantly higher myocardial count rate (7 to 8 times), compared with conventional single-photon emission tomography (SPECT) at stress and rest images. CPM, Counts/minute. Reproduced with permission.

MULTI-PINHOLE COLLIMATION APPROACH

Some vendors have explored image collimation using multi-pinhole design. Multi-pinhole collimation provides an alternative approach to parallel-hole

rotational tomography. Previously, useful results have been demonstrated in small animal imaging with multi-pinhole SPECT providing improved spatial resolution and detection efficiency in comparison to parallel-hole collimation.¹⁸⁻²⁰ The multi-pinhole approach allows many views to be acquired simultaneously throughout the entire image acquisition period without the need for motion of the detector, collimator or patient. This capability allows image acquisition to be accomplished without the need for any electro-mechanical hardware, potentially reducing the manufacturing and servicing costs. In addition to the increase in detection sensitivity, the use of stationary detectors equipped with multi-pinhole collimation provides coincident sets of raw images eliminating view-to-view inconsistencies and thereby reducing artifacts induced by patient motion. Therefore, by the multi-pinhole approach, all views are active for the entire acquisition period providing a compatible dataset for input to iterative SPECT reconstruction algorithms.

However, multi-pinhole design potentially suffers from limitations which will need to be addressed. The approach may be prone to greater formation of artifacts

because it inherently produces an incomplete tomographic dataset and it acquires images from only limited views.²¹ Background activity from other organs may not be seen by all of the views, which could lead to inconsistencies in the reconstructed data. It is also known that the resolution and sensitivity of pinhole collimators decreases with the distance from the collimator²²; however, there is the potential that resolution recovery can be applied during the reconstruction to compensate for this spatial variation.

Clinical multi-pinhole imaging systems for optimized MPS imaging have been developed recently by Eagle Heart Imaging (Westminster, Colorado) as an add-on to standard cameras and by General Electric combined with dedicated solid-state detectors and are described in the following sections.

EAGLE HEART IMAGING

Existing SPECT systems with one or more large-area detectors are potentially adaptable to the stationary multi-pinhole SPECT approach. Eagle Heart Imaging (Westminster, Colorado) has integrated multi-pinhole methodology with the Emory Reconstruction Toolbox (Syntermed, Atlanta, GA) to provide a commercial multi-pinhole upgrade product called MP-SPECTTM for existing dual-head SPECT gamma cameras.

Figure 10 illustrates an approach for upgrading a standard dual-detector SPECT camera for imaging the human heart by multi-pinhole SPECT technique. The performance characteristics for a multi-pinhole SPECT system applicable to cardiac imaging were reported by Funk et al²¹ using a 9-pinhole collimator design applied using a 1, 2, or 4 detector configuration. In experiments with an initial prototype system, the authors found that the spatial resolution of the 9-pinhole collimator using 8-mm-diameter pinholes was 30% less than that achieved by standard parallel-hole collimation. However, the detection efficiency was increased 10-fold. These data predict a 5-fold increase in sensitivity and would provide comparable resolution to that of a standard gamma camera. A similar increase in detection sensitivity has been reported by the same group for a full ring, small animal multi-pinhole SPECT system.²³

Another issue addressed by Funk et al²¹ concerns the minimal number of views and the optimal viewing geometry required for clinical cardiac SPECT. There are both advantages and disadvantages to having fewer views. As the number of views present in the SPECT data set is decreased, the geometric appearance of the heart is visibly altered. This aspect must be weighed against the fact that the increased statistical content and simultaneity of these views improves the comparability of the stress versus rest data sets acquired on the same

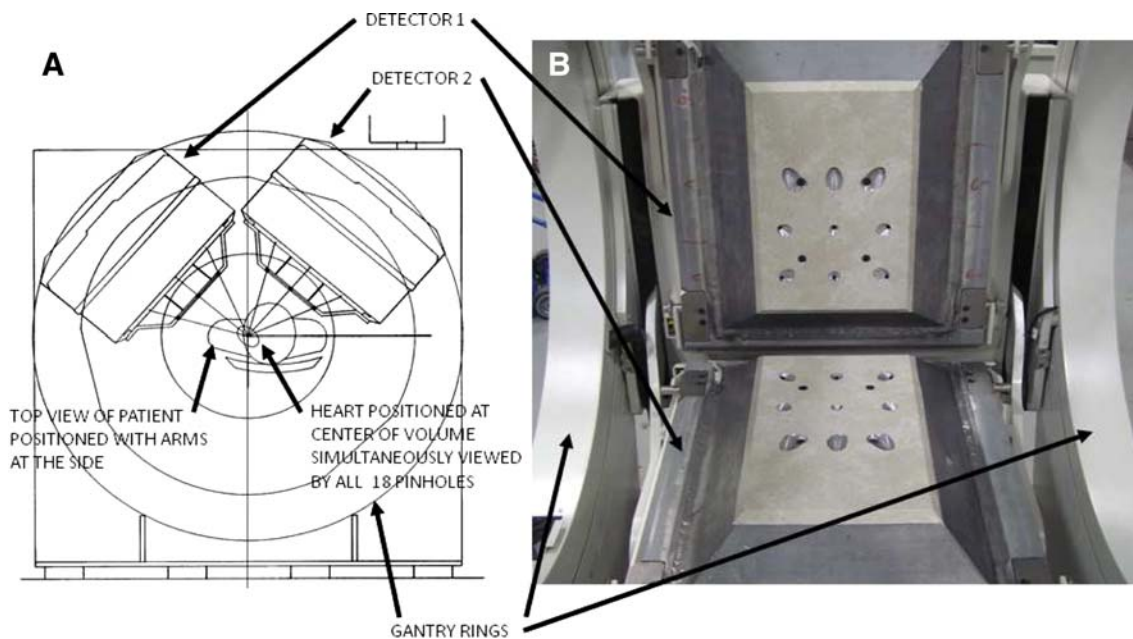


Figure 10. Illustration of a multi-pinhole upgrade to an existing commercially available dual-head gamma camera system. **A**, Diagram looking longitudinally toward the patient's feet. **B**, Photograph taken from the patient's perspective showing the pair of 9-pinhole collimators of the dual-detector MP-SPECTTM upgrade. Images courtesy of Dennis Kirch (Eagle Heart Imaging, Westminster, CO).

patient. The improved statistical content of multi-pin-hole SPECT images is also a key factor in supporting the ability to image multiple isotopes simultaneously. The clinical utility of this approach has been reported by Steele et al²⁴ who demonstrated clinical comparability between a three detector 18-pin-hole SPECT system and a conventional rotational SPECT gamma camera.

Reconstructed images in slice format developed by Eagle Heart Imaging are shown in Figure 11A and the corresponding polar perfusion maps are displayed in

Figure 11B. The results of breath-by-breath motion correction are shown in Figure 12.

GE HEALTHCARE ULTRA FAST CARDIAC (UFC) CAMERA

General Electric Healthcare recently (SNM 2008) introduced the UFC camera based on the multi-pin-hole design and an array of cadmium zinc telluride (CZT) pixilated detectors. The camera has received 510(k)

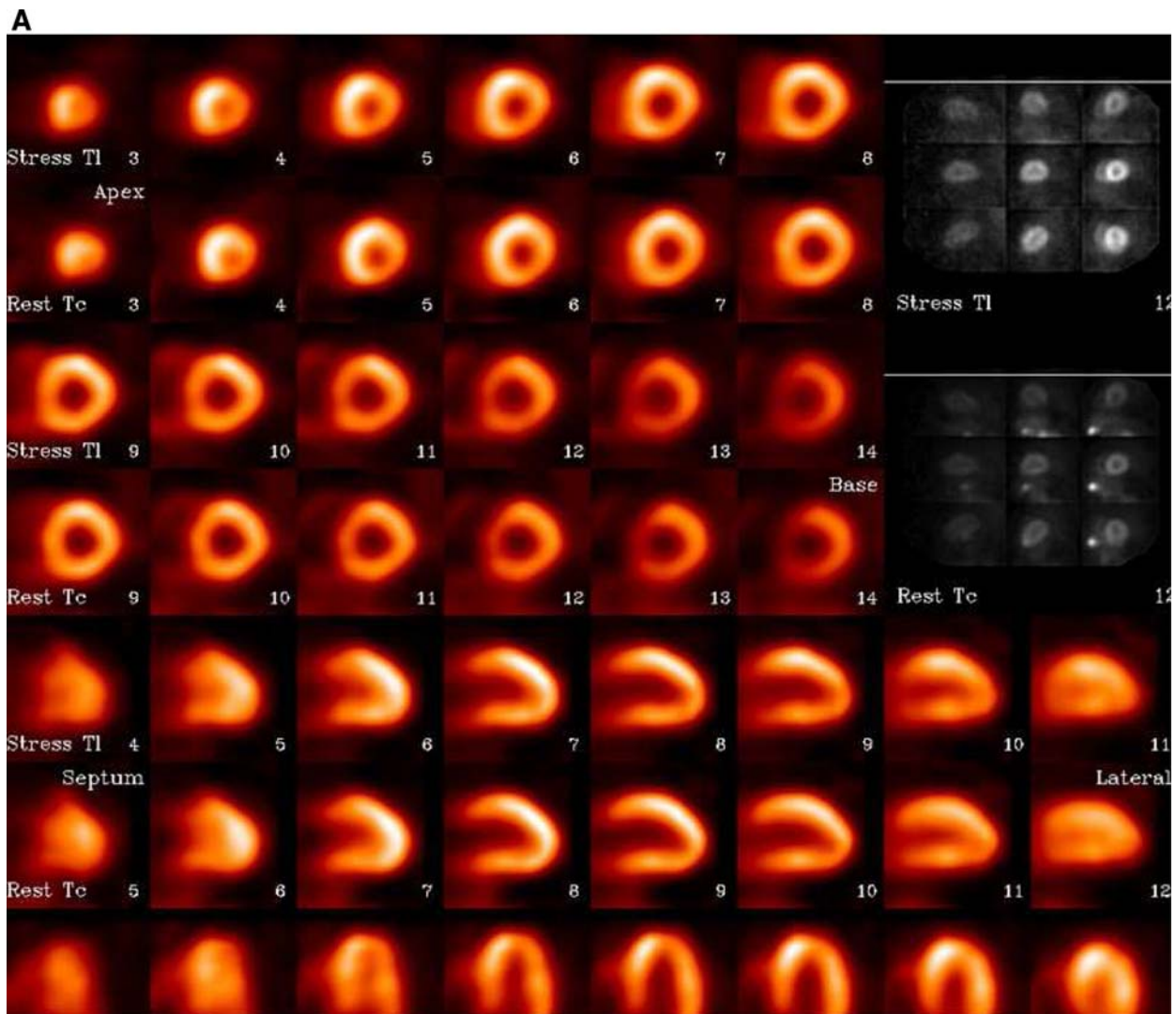


Figure 11. Reconstructed short- and long-axis slices for an MP-SPECTTM study in which the resting Tc-99m images and the stress Tl-201 images were acquired simultaneously. Image acquisition time was 15 minutes. The *black-and-white* images in the upper right-hand corner are the raw 9-pin-hole projections for detector 2 for each isotope (Tc-99m for rest and Tl-201 for stress) (A). Stress and rest polar perfusion maps developed from the MP SPECTTM reconstructions (B) do not show significant (>10%) differences as seen in the lower right-hand map. Images courtesy of Dennis Kirch (Eagle Heart Imaging, Westminster, CO).

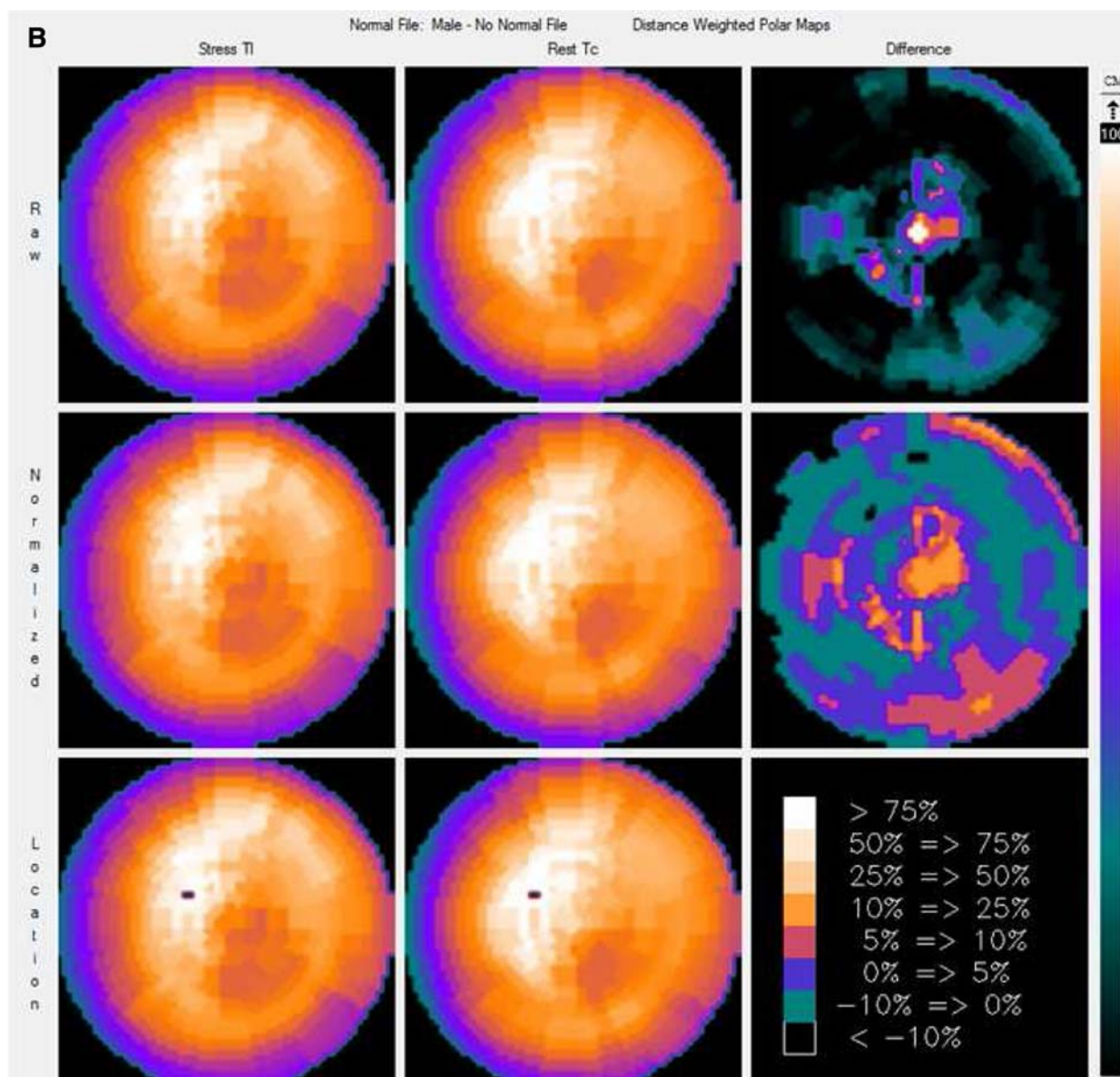


Figure 11. continued.

clearance from the U.S. Food and Drug Administration (FDA) and is manufactured by GE Healthcare. The use of CZT improves the energy and spatial resolution while the use of simultaneously acquired views improves the overall sensitivity and gives complete and consistent angular data needed for both dynamic studies and for the reduction of motion artifacts. In this system, the detectors and collimators do not move during acquisition and all lines of response are acquired simultaneously through a proprietary multi-pinhole collimator with a large number of pinholes. Patients are imaged in a supine position with their arms placed over their heads. The design of the UFC camera is shown in Figure 13. It has

been shown that for fixed energy acceptance windows, the asymmetric CZT energy response shape leads to a 30% reduction of the scatter component in measured data.²⁵ It has been also shown that the combination of CZT with a pinhole collimator is seen to further enhance the improved energy resolution available as compared to from CZT alone,²⁶ which may facilitate new applications such as simultaneous dual isotope imaging. GE uses maximum a posteriori (MAP) iterative reconstruction adapted to the UFC geometry.

Three institutions (Emory University in Atlanta; the Mayo Clinic in Rochester, MN; and Rambam University in Haifa, Israel) collaborated in clinical trials reporting

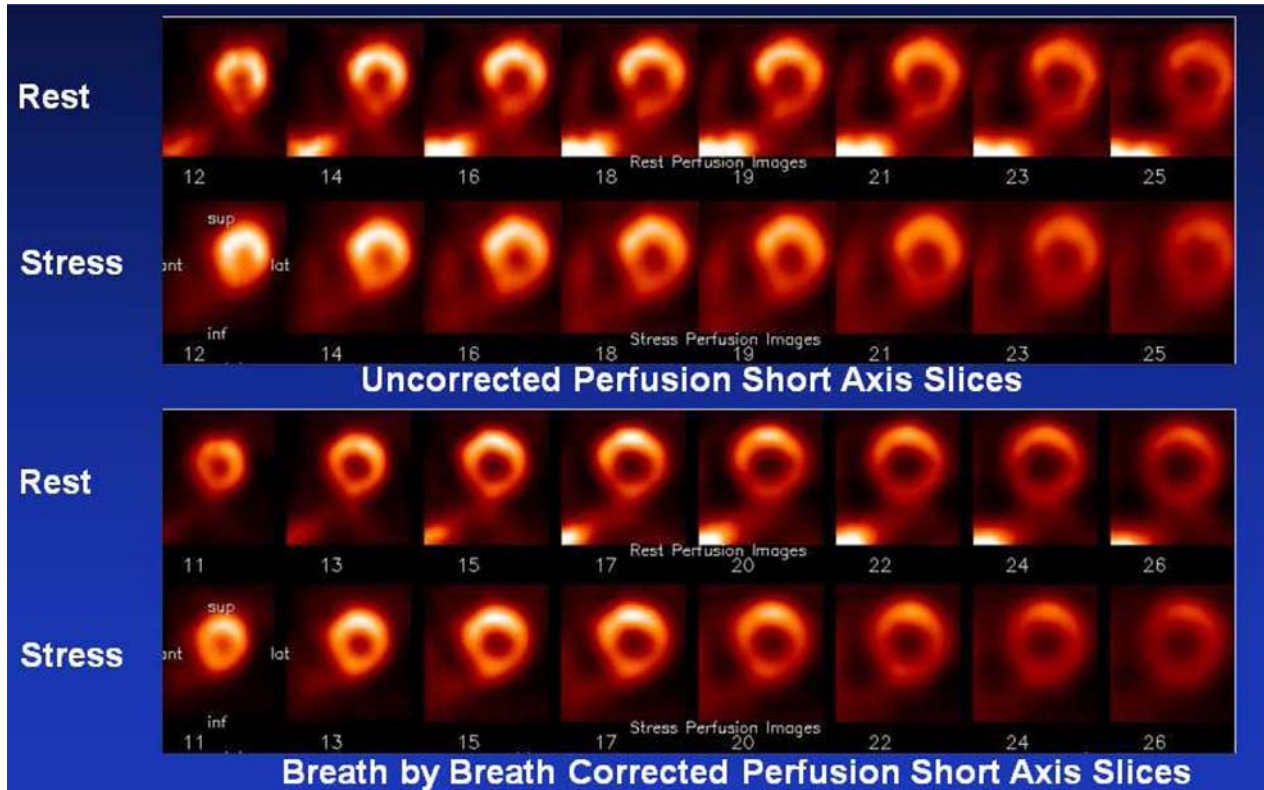


Figure 12. Short-axis reconstructed MP-SPECT™ images before (*above*) and after (*below*) correction for respiratory motion. The correction algorithm applied here breaks the list-mode acquisition into segments corresponding to individual R-to-R wave intervals and the image segment for each beat is shifted so that the centers-of-mass superimpose. Images courtesy of Dennis Kirch (Eagle Heart Imaging, Westminster, CO).



Figure 13. The photograph of the GE Healthcare Ultrafast Cardiac camera. Images courtesy of Frank Antsett, GE Healthcare.

preliminary data from 126 patients in which imaging was done in sequence with the same injected dose with standard GE Ventri camera (12-17 min stress and 12-

14 minute rest acquisitions) and UFC camera (4 minute rest 2 minute stress acquisitions) with an equivalent imaging protocol and reported that 85% of UFC scans were rated as “excellent,” compared to 63% with the standard SPECT camera. Also, in a recent preliminary report, compared to the standard, state-of-the-art SPECT camera Ventri, UFC demonstrated improvements of 1.65-fold in energy resolution, 1.7-2.5 fold in spatial resolution and 5-7 fold in sensitivity with UFC energy resolution of 5.70% and spatial resolution in the 4.3-4.9 mm range.²⁷ Typical clinical images obtained by UFC camera are shown in Figure 14.

SIEMENS IQ•SPECT

Siemens introduced recently (SNM 2008) IQ•SPECT, which consists of three components: an astigmatic collimator, an optimized organ-of-interest centered acquisition, and iterative reconstruction. The collimator is based on a previously developed astigmatic (cardiofocal) collimator concept.²⁸ The collimator is designed so that the center of the field-of-view magnifies the heart both in axial as well as in trans-axial direction,

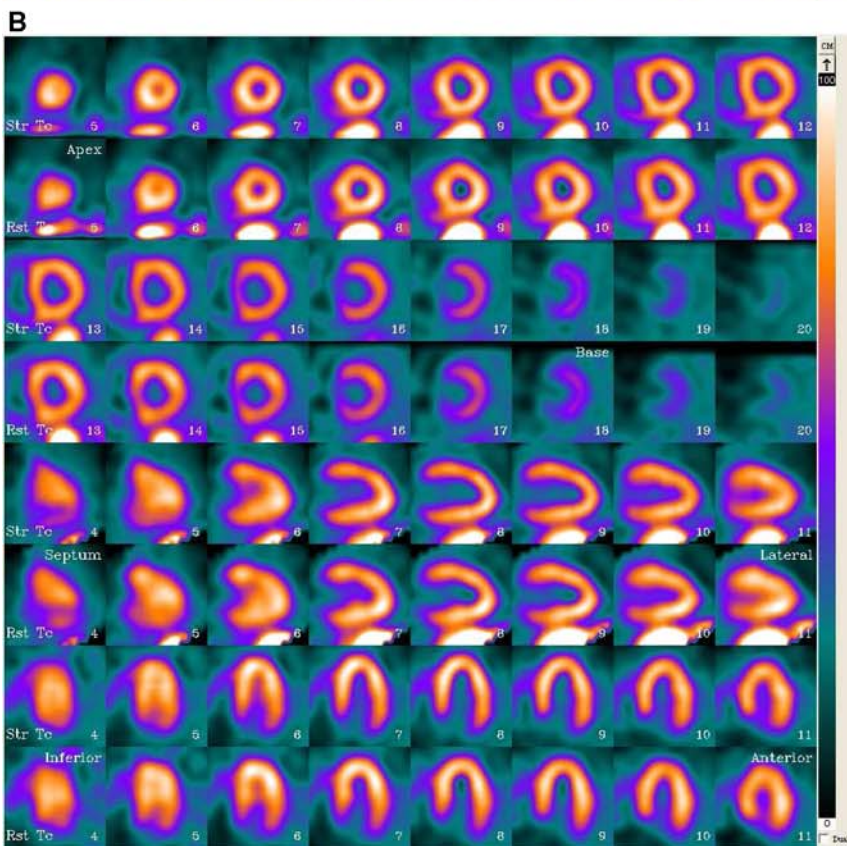
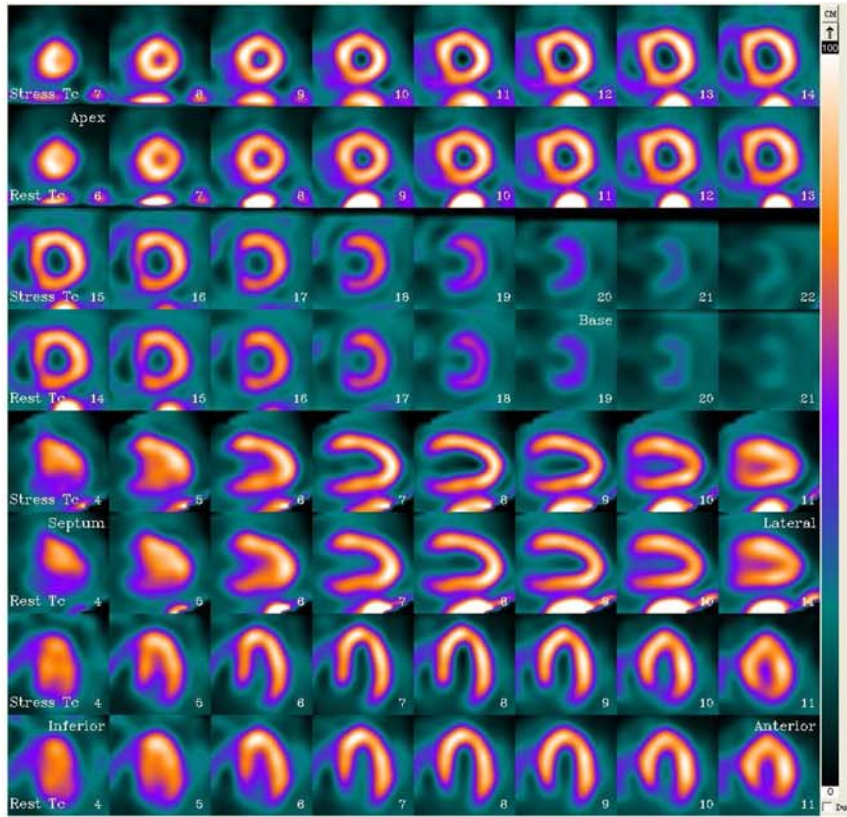


Figure 14. Results from a normal patient who underwent rest/stress Tc-99m tetrofosmin myocardial perfusion imaging using 10 mCi for rest and 30 mCi for stress. The figure shows short, vertical, and horizontal oblique axis slices starting with stress images in the first row and immediately below the corresponding resting images. Rest and stress acquisitions were 4 and 2 minutes, respectively, for UFC camera and 14 and 12 minutes, respectively, for conventional CardioMD SPECT system. UFC images are shown in (A) and standard images are shown in (B). Images courtesy of Dr. Ernest V. Garcia, Emory University, Atlanta, GA.

while the edges sample the entire body to avoid truncation artifacts common to single focal collimators when imaging the torso. With an appropriate orbit this variable-focus collimator increases the number of detected events from the heart by more than a factor of two in each direction compared to that of a parallel-hole collimator with equivalent resolution, and magnifying the heart while imaging the rest of the torso under traditional conditions.²⁸ The principle of image acquisition with these collimators is shown in Figure 15. Traditionally, MPS data are obtained by keeping the detectors positioned at 90° and as close to the body as possible, and utilizing mechanically centered detector rotation, where organ-specific magnification cannot be achieved. Symbia S and T Siemens gantries allow an organ centric detector rotation, where the principal ray of the collimators intersect the organ of interest in all views and maintaining a constant radius of rotation about that center; in this case, the heart.

In IQ•SPECT this organ centric orbit acquisition technique is combined with a new proprietary iterative reconstruction algorithm based on Flash3D^{29,30} (see also the section on image reconstruction) which models the

astigmatic geometry of these collimators. IQ•SPECT reconstruction also includes state-of-the-art distant-dependent isotropic (3D) resolution recovery, CT-based attenuation correction, and energy window-based scatter correction. The reported image acquisition time of this system can be as short as 4 minutes. These collimators are offered as an upgrade to the existing Symbia line of cameras.³¹ The Symbia T series systems also allow for obtaining of CT calcium scan in as little as 30 seconds during the same imaging session, where the CT data could be also used for attenuation correction. Figure 16 shows an example of a clinical 4-minute stress and 4-minute rest MPS scan with CT attenuation correction obtained with Symbia T camera equipped with IQ•SPECT technology.

RECONSTRUCTION ALGORITHMS FOR FAST IMAGING WITH STANDARD MPS SYSTEMS

Faster MPS imaging can be also accomplished by advanced image reconstruction techniques, which improve image contrast and reduce noise levels inherent in images with low counts reconstructed with filtered

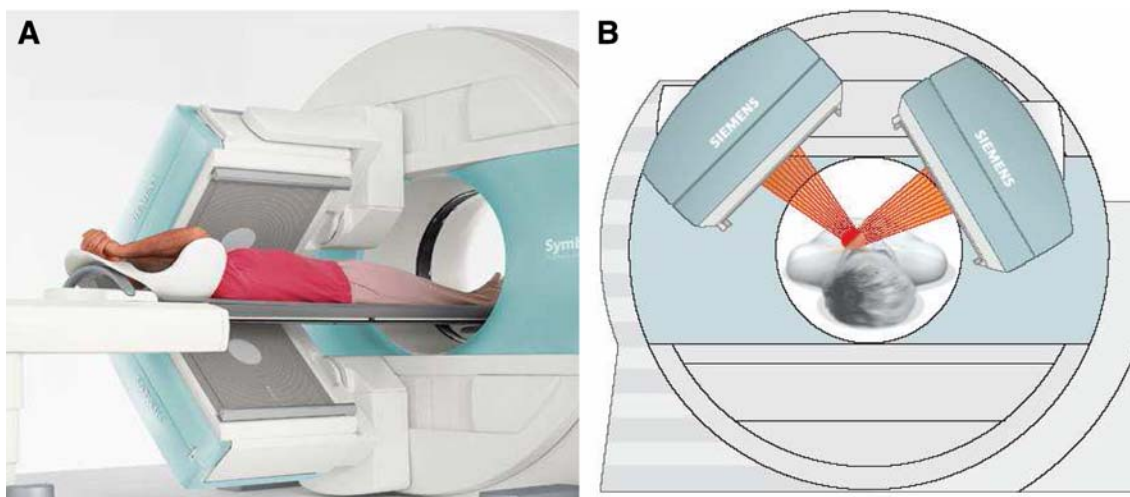


Figure 15. The photograph (A) and the collimation design (B) of the SMARTZoom Siemens collimators. The astigmatic collimator is designed to achieve a 2× magnification of the heart in all directions and thus a 4× sensitivity increase for the heart region without truncation of the torso in a specified orbit. In the specified orbit, the detector heads are positioned at 76°, keeping a fixed radius of 28 cm about the “center of rotation” which now is located in the heart region. The scan range is 208°, combining views from both detectors. Images courtesy of Siemens Medical Solutions USA, Inc.; Molecular Imaging, Hoffman Estates, IL.

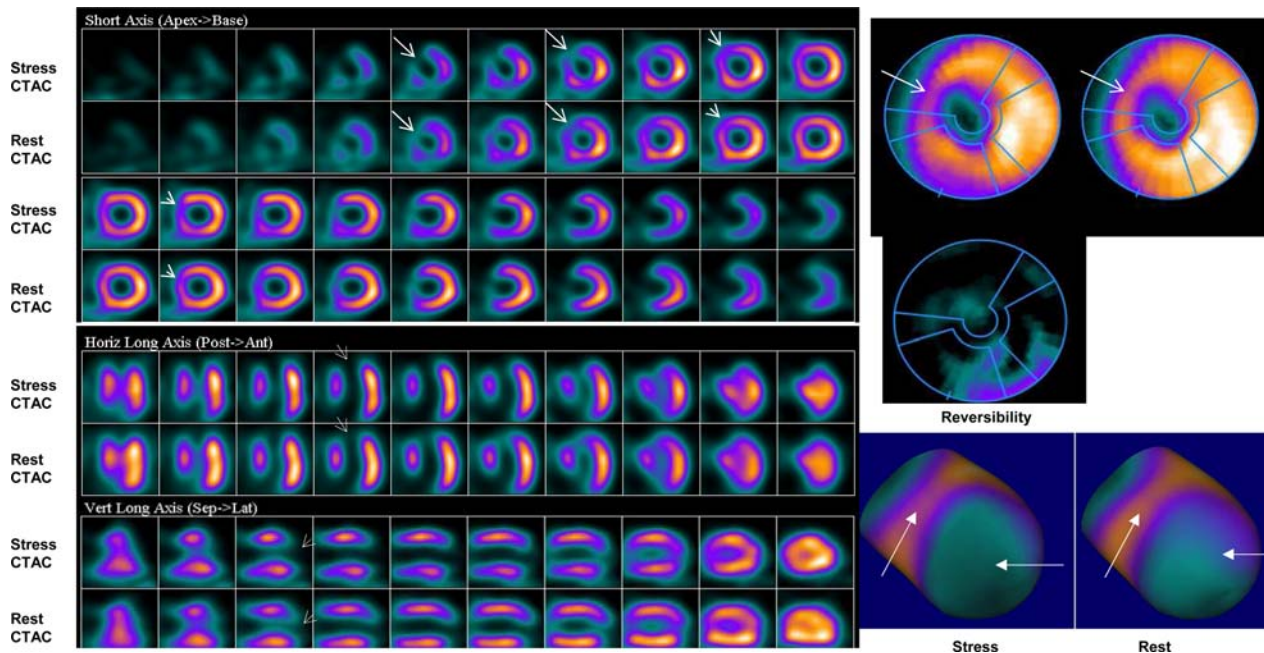


Figure 16. A 65-year-old male patient with a history of myocardial infarction underwent 99m-Tc MIBI MPS scan on Symbia T6 IQ•SPECT with treadmill (stress dose 7 mCi 99m-Tc MIBI followed by rest dose 22 mCi after 3 hours). Integrated low-dose CT was performed during free breathing and used for CT attenuation correction. The study shows a large fixed perfusion defect in the anterior wall, apex and septum related to previous infarction and a slight amount of reversible ischemia in the peri-infarct zone, distal septum and inferior wall. Stress and rest study were acquired in 4 minutes each. Images courtesy of Siemens Medical Solutions USA, Inc.; Molecular Imaging, Hoffman Estates, IL.

back-projection (FBP). These developments have centered on the development of new proprietary algorithms based on maximum likelihood expectation-maximization (MLEM)^{32,33} and accelerated method of ordered subsets expectation maximization (OSEM).³⁴

FBP reconstruction assumes that the object is detected equally in all of the angular projections. This leads to various artifacts caused by variations in attenuation, scatter, resolution, and count density. Iterative MLEM and OSEM reconstruction methods allow the geometry of the acquisition to vary for each projection, greatly enhancing the flexibility in modeling the physical parameters. MPS is significantly affected by Poisson noise, scatter, attenuation correction, and variable image resolution³⁵ but the iterative methods allow incorporation of accurate corrections for these degrading factors into the reconstruction process, so that the reconstructed image is a better representation of the object being imaged.

Currently, the most widely used iterative technique is based on the OSEM approach, which is an accelerated version of the MLEM algorithm. This technique groups projection data into an ordered sequence of subsets for efficient computation. One iteration of the OSEM

algorithm is defined as a single pass through all of the subsets.³⁴ Typically, 2-4 projections per subsets are used, with 4-12 iterations, which is computationally less demanding than 1 iteration of standard MLEM algorithm (assuming 64 projections). Even with 1 iteration of OSEM and 32 subsets it is possible to obtain a reasonable initial reconstruction. Typically, OSEM results in an order of magnitude decrease of computing time without measurable loss of image quality, as demonstrated by Hudson et al.³⁴ Computational efficiency of OSEM allows for incorporation of more complicated modeling during the reconstruction process. In OSEM, reconstruction image data are updated for each subset during each iteration. Therefore, the number of updates is the product of iterations and projections subsets. As the number of updates increases, the spatial resolution increases; however, with increasing noise, which necessitates an optimization process where the noise smoothing filter, the number of iterations, and the number of subsets are properly balanced in order to obtain optimal image quality, i.e. spatial resolution and uniformity. Therefore, most current algorithms utilize various forms of noise suppression during iterative reconstruction.

Scatter and attenuation compensation can be integrated within iterative reconstruction. In addition, resolution recovery techniques can be incorporated to correct for losses in spatial resolution due to image blurring by the collimator.³⁶ The current algorithms simultaneously address these problems by modeling the instrumentation and imaging parameters used for a specific application in order to eliminate the degrading physical effects and suppress noise in the image reconstruction process. The resolution recovery aspects of these algorithms can be emphasized to provide significant improvements in spatial resolution and MPS image quality, and the noise suppression aspects can be emphasized to decrease imaging times.

PHILIPS ASTONISH

Philips (San Jose, CA) has developed a fast SPECT reconstruction algorithm (Astonish) that includes corrections for the major factors degrading SPECT image quality. It is based on the OSEM reconstruction method with built-in noise reduction methods during the iterative process, and incorporating corrections for photon scatter, photon attenuation, and variations in spatial resolution. Correction for Compton scattering in the patient improves lesion contrast and is required for accurate attenuation correction. Correction for photon attenuation provides a more accurate representation of the counts from lesions that are at different depths inside the patient. Correction for variations in spatial resolution with depth allows the preservation of sharper details and small lesions with greater conspicuity. The company has developed this approach to shorten the MPI acquisition time without compromising the image quality.

The corrections for variations in spatial resolution use measurements of the changes in spatial resolution with distance from the collimator. Calibrations for each of the collimators are measured initially by the manufacturer. Astonish software incorporates this collimator information both into the back projection and the forward projection parts of the reconstruction. The resolution recovery correction in Astonish can be performed with or without attenuation and scatter corrections.

In Astonish, the corrections for the photon scatter are performed by the ESSE method described by Kadmas et al.³⁷ The corrections for the photon scatter are performed prior to the attenuation correction in each iterative OSEM step. Corrections for attenuation are performed during the forward projection process. Attenuation correction requires knowledge of both the photon attenuation coefficient and the density of each pixel that the “counts” are forward projected through. The density information is accessed in an attenuation

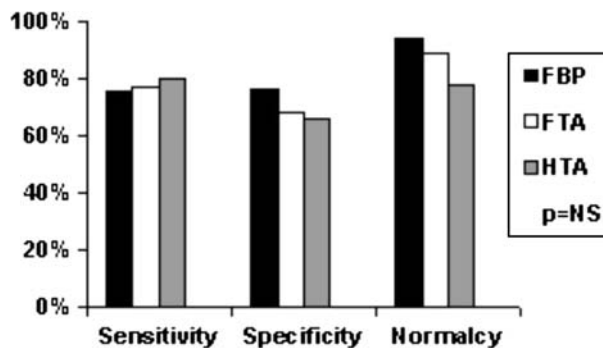


Figure 17. The sensitivity, specificity, and normalcy were determined for filtered back projection (FBP), full-time Astonish (FTA), and half-time Astonish (HTA). Figure courtesy of Gary Heller University of Connecticut School of Medicine CT⁴².

map, modified from a previously acquired density image, either with a scanning line source or with a CT scanner.

To avoid amplification of statistical noise during the reconstruction process, Astonish uses a proprietary (patent pending) noise reduction method of smoothing both the estimated projection data and the measured projection data internally during the reconstruction process^{38,39} using an optional Hanning filter. This modification of OSEM allows for optimized control of Poisson image noise while maintaining higher image resolution. The estimated projections are also smoothed with the same filter prior to the measured/estimated comparison being taken during each subset. This approach can be compared with other methods that smooth the image data after the reconstruction process.⁴⁰

Astonish technique has been tested in a multi-center trial consisting of 221 patients, and preliminary results have been reported.⁴¹ The half-time Astonish data were obtained by simulation from the full-time data by using half of the original projections. Interpretative certainty and diagnostic accuracy (Figure 17) were the same for standard FBP reconstruction, full-time Astonish and half-time Astonish. An example of MPS image quality achievable with Astonish is shown in Figure 18. In addition, this technique has been applied to perform stress only fast imaging with attenuation correction and preliminary study confirmed equivalent diagnostic results to the standard stress/rest scans reconstructed with FBP.⁴²

GENERAL ELECTRIC HEALTHCARE—EVOLUTION SOFTWARE

General Electric Healthcare, Waukesha, WI, has developed a modification of the OSEM algorithm which incorporates resolution recovery or OSEM-RR

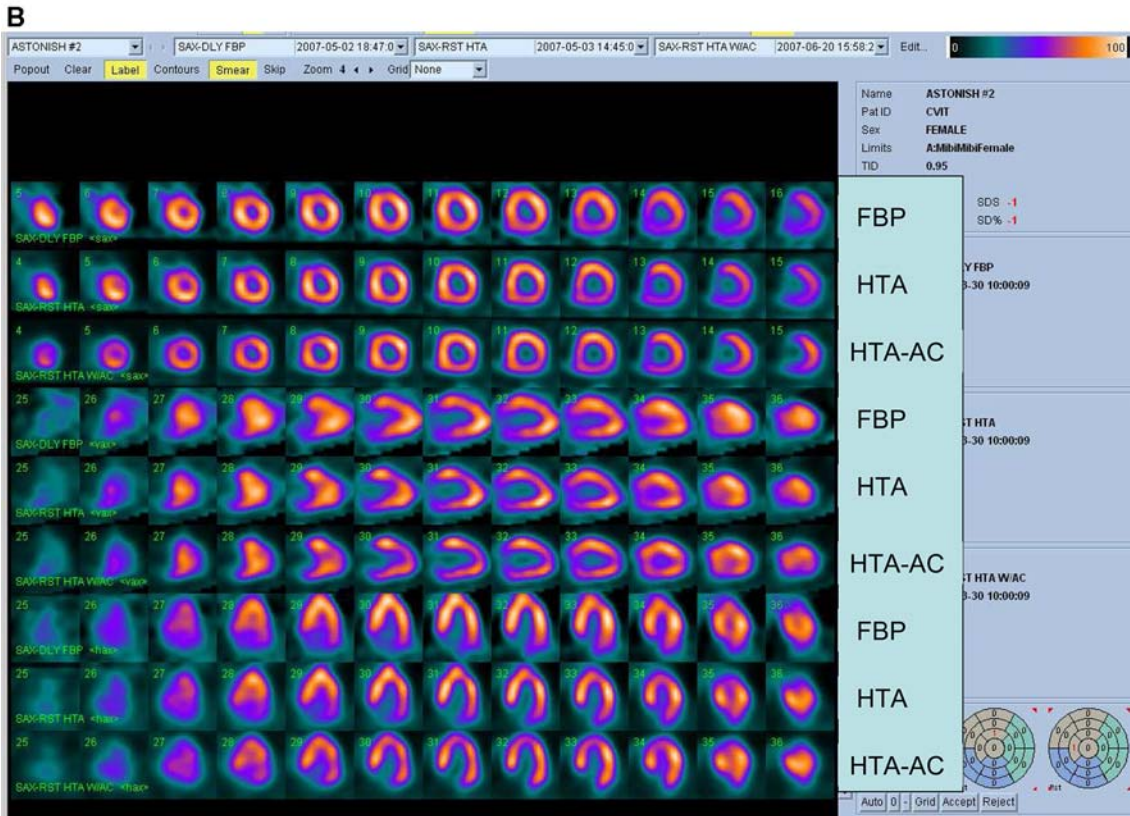
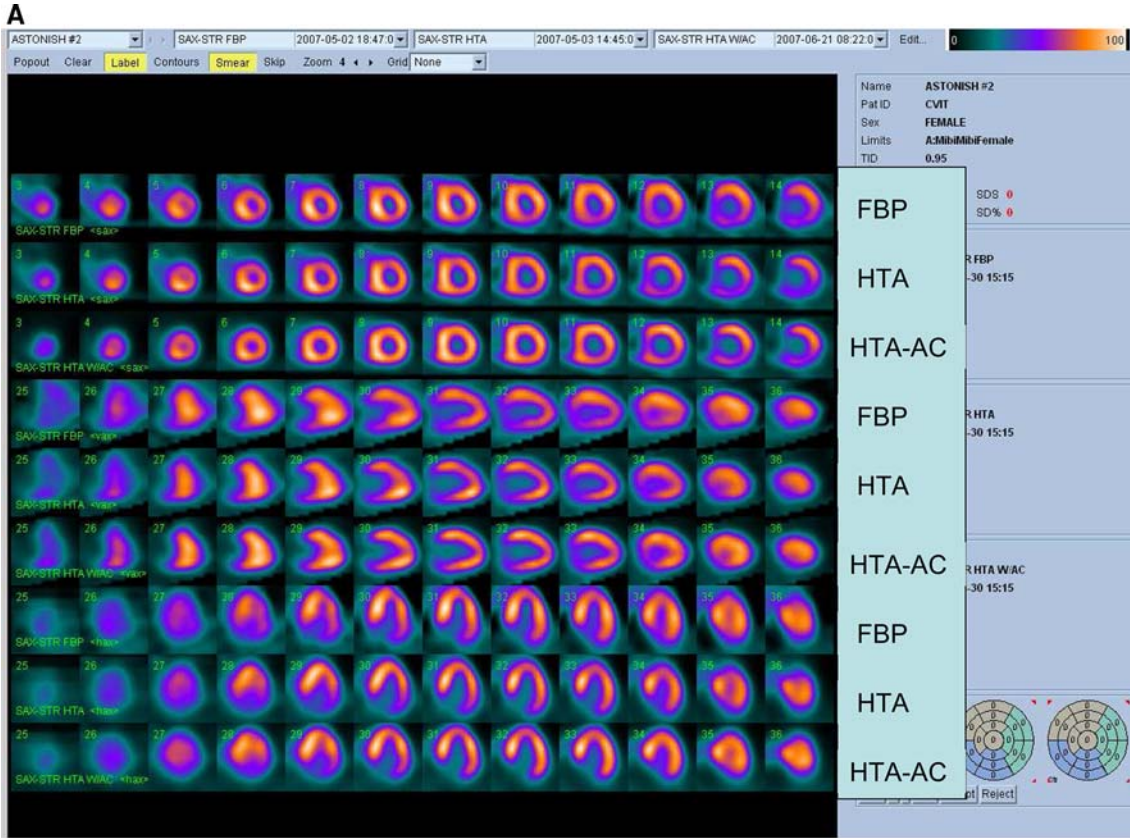


Figure 18. Example of image quality with Astonish. Stress (A) and rest (B) images are reconstructed with standard FBP image reconstruction (FBP), Half-time Astonish reconstruction (HTA) and half-time Astonish reconstruction with attenuation correction (HTA-AC). Images of a 209 lbs male were acquired with a Tc/Tc protocol with 64 projections and 25 seconds per view (full time), and with 32 projections and 25 seconds per view (half time), acquired on Cardio MD Philips camera. Images courtesy of Philips Healthcare.

(Evolution for Cardiac). Their approach includes modeling of the integrated collimator and detector response function (CDR) in an iterative reconstruction algorithm and performs image resolution recovery⁴³ based on these parameters. This technique has been described in detail by DePuey et al.⁴⁴ The OSEM-RR modeling includes basic collimator geometric response function for round-hole-shaped collimators^{36,45} which can be applied with good approximation to hexagonal holes.

The CDR compensation technique utilized in OSEM-RR was developed at the University of North Carolina Chapel Hill and Johns Hopkins University by Tsui et al.^{43,45,46} It is accomplished by convolving the projected photon ray with the corresponding line spread function (LSF) during iterative projection and back-projection. The following parameters are accounted for and compensated: collimator hole and septa dimensions, intrinsic detector resolution, crystal thickness, collimator to detector gap, and projection-angle specific center-of-rotation to collimator face distances. These collimator-specific data are embedded in the software in the form of look-up tables. Some of the relevant acquisition parameters (such as object to collimator distance) are obtained directly from the raw projection data.

Additionally, similar to other optimized reconstruction methods, OSEM-RR incorporates noise suppression, which is required since the resolution recovery during iterative reconstruction process amplifies noise which can lead to the formation of hot spots in the final image. An MAP technique⁴⁷ is incorporated to control image noise in the OSEM-RR design. A modified one-step-late algorithm with a Green prior⁴⁸ is utilized. The specific parameters in these reconstructions are optimized separately for each clinical protocol, and separately for gated and attenuation corrected images. The last iteration is performed using a Median root prior.⁴⁹

SIEMENS FLASH 3D

Siemens has developed software (Flash3D) incorporating iterative fast OSEM reconstruction with 3D resolution recovery, 3D Collimator and Detector Response Correction, and attenuation and scatter compensation.⁵⁰ SPECT cardiac acquisition protocols (CardioFlash) have been developed utilizing Flash3D, where the acquisition time can be reduced to between 33% and 50%, as compared to the standard acquisition

protocols with FBP reconstruction. An example of the image quality obtained with CardioFlash is shown in phantoms (Figure 19) and in clinical images (Figure 20). To date, it has been shown, in phantom data in combination with few clinical scans, that Flash3D allows faster acquisition protocols but still provides sufficient myocardial uniformity and lesion detectability.⁵⁰ A preliminary report of a study of myocardial

Torso Phantom normal (33kcts/view; 64² 4.8 mm)

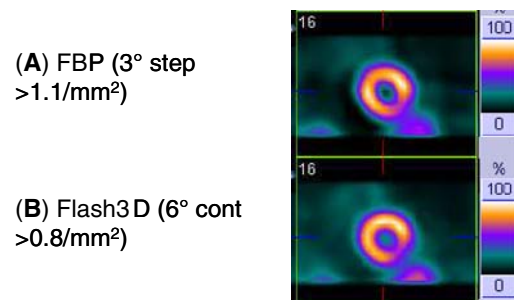


Figure 19. Example images comparing a standard protocol and a protocol using Flash3D in 36% of the acquisition time. The infero-lateral artifact due to lack of attenuation correction is well visible in phantoms. Reproduced with permission from Vija et al⁵⁰.

Example Patient data (rest, 64², 6.6 mm)

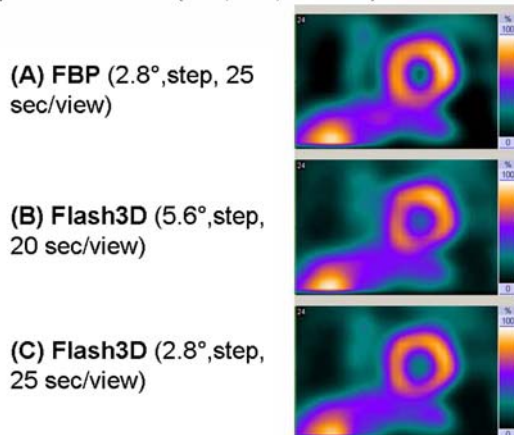


Figure 20. Example patient data acquired with CardioFlash. For images (A) and (C) the original projection data are used, but reconstructed with FBP and Flash3D. The projection data in (B) are extracted from the original data and represent a “what-if” protocol dataset with twice the angular step size and 80% dwell time reduction, and reconstructed with Flash3D. Reproduced with permission from Vija et al⁵⁰.

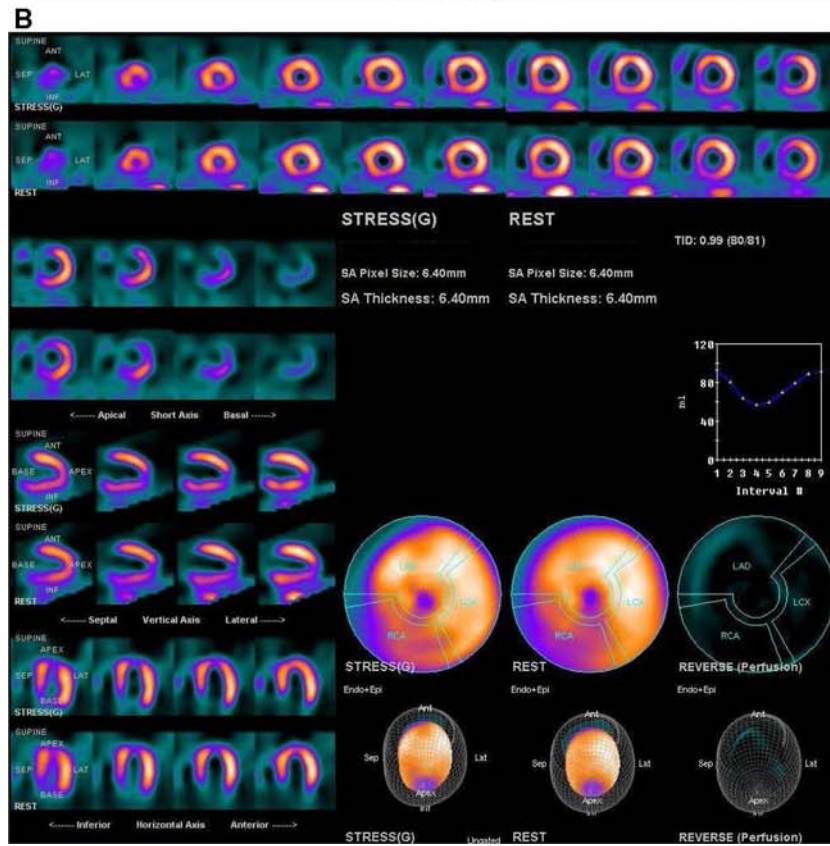
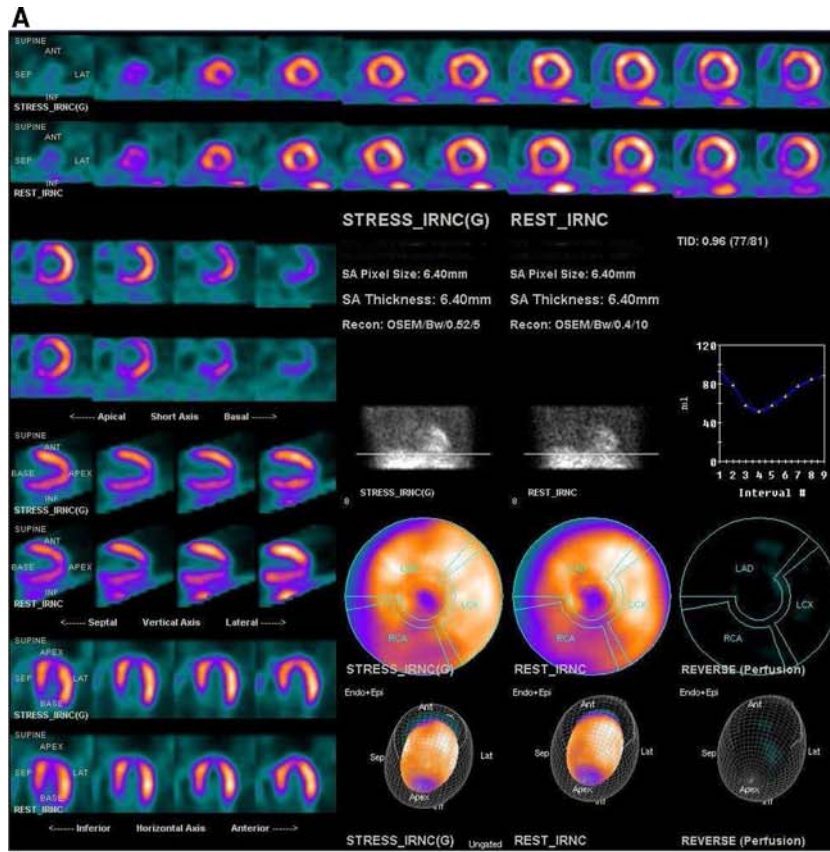


Figure 21. SPECT scans of a 56-year-old male hypertensive smoker with no prior history of coronary disease. Images obtained with Tc-99m sestamibi (dose: 8 mCi at rest and 32 mCi at stress) protocol and acquired with dual-head scintillation camera without attenuation correction. Images were reconstructed with full-time OSEM (15 minutes rest and 12 minutes stress) (A) and with separate wide beam reconstruction (WBR™) (9 minutes rest, 7 minutes stress) acquisitions (B) following the rest and stress OSEM acquisitions, respectively. The actual acquisition time for “half time” WBR is slightly longer than 1/2 due to the dead time associated with gantry rotation. However, the WBR acquisition time per camera stop is one-half that for OSEM. Both WBR and OSEM images show the same small apical defect which is likely physiological apical thinning. Images courtesy Dr. Gordon DePuey, Columbia University, New York City.

perfusion distribution in normals with half-time Flash3D imaging has been recently presented by the University of Michigan group.⁵¹ They found that, in normal patients, Flash3D can handle imaging times reduced to 50% with no change in the normal perfusion distribution.

The computer reconstruction times of the 2007 release of Flash3D (Siemens’ OSEM reconstruction with 3D distance dependent resolution recovery and optional scatter and attenuation corrections) have been improved, and it is now possible to process an entire clinical gated cardiac dataset in less than one minute on a standard workstation. High correlation ($r^2 > .97$) has been shown between the ejection fractions obtained from conventional FBP-based protocol and the Cardio-Flash reconstructions in a preliminary study.⁵²

ULTRASPECT WIDE BEAM RECONSTRUCTION

UltraSpect, Inc. (Haifa, Israel) has developed a standalone workstation (Xpress.cardiac) which utilizes the patented wide beam reconstruction (WBR™) algorithm.⁵³ The WBR reconstruction technique, phantom validation, and its clinical application have been recently described by Borges-Neto et al.⁵⁴ This system is available as an additional workstation and can reconstruct data from most existing gamma cameras with standard collimators. WBR models the physics and geometry of the emission and detection processes and attempts resolution recovery. During the iterative reconstruction it uses the information regarding the collimator’s geometry (such as the dimensions and shape of holes or the septa thickness) and the detector’s

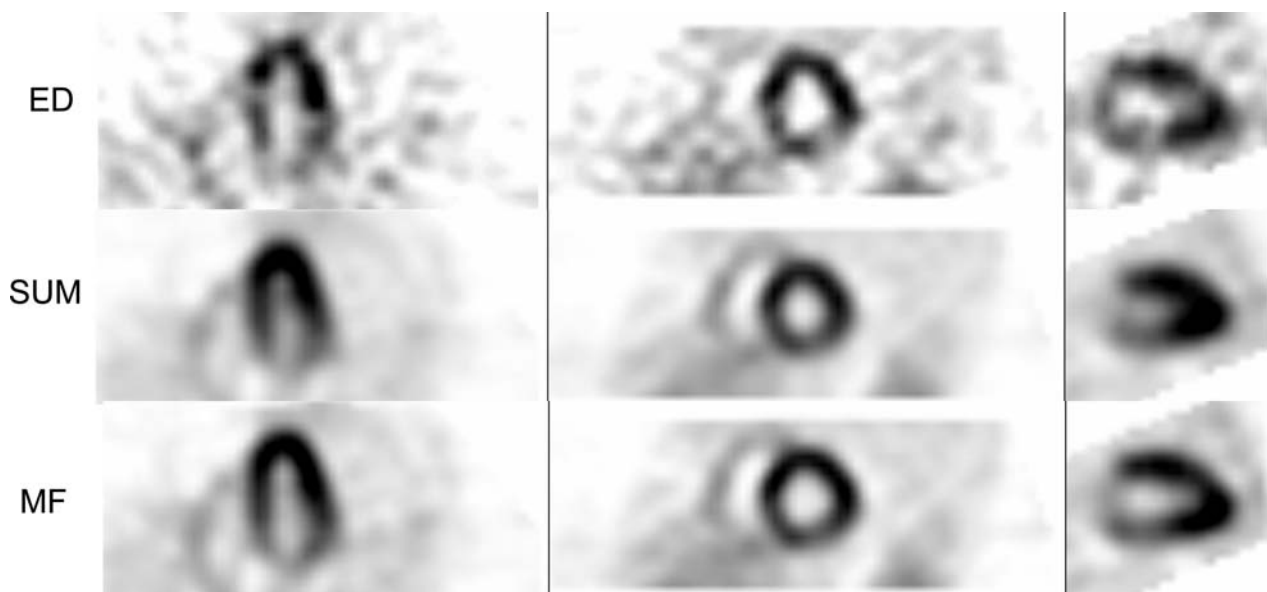


Figure 22. Short axis and vertical long axis of motion frozen (MF) reconstruction and standard summed reconstruction (SUM) of gated SPECT images. Motion-frozen perfusion images compared to the summed perfusion images in the case of double vessel disease confirmed by angiography (100% LAD occlusion and 80% LCX occlusion). Both standard quantification technique and visual analysis of summed data identified only the LAD lesion; the additional LCX lesion was identified only by the “motion-frozen” quantification. Reproduced with permission from Slomka et al.⁵⁶

distance from the patient. This distance can be obtained automatically on new cameras but also can be obtained by image processing techniques and definition of the 3D patient body contour from standard images.⁵⁴ To determine the approximate noise level that is present in the acquired data, WBR applies statistical modeling of the expected photon emission and Fourier analysis of projection data. This allows selection of an optimal noise model to yield the appropriate balance between resolution and noise. An example of WBR image quality is shown in Figure 21. Recently, a preliminary study of WBR demonstrated equivalent image quality and defect characterization with simulated fast imaging with times as low as one-fourth of standard imaging time as compared to full-time standard reconstruction.⁵⁵

MOTION-FROZEN RECONSTRUCTION

A related technical development resulting in improved MPS image quality is the “motion-frozen” processing of gated cardiac images, which eliminates blurring of perfusion images due to cardiac motion.⁵⁶ This technique applies a non-linear, thin-plate-spline warping algorithm and shifts counts from the whole cardiac cycle into the end diastolic position. The “motion-frozen” images have the appearance of ED frames but are significantly less noisy since the counts from the entire cardiac cycle are used. The spatial resolution of such images is higher than that of summed gated images. This technique has been successfully applied to SPECT and PET images. Figure 22 shows an example of SPECT image reconstructed with motion-frozen technique. A significant improvement in image resolution can be observed as compared to the standard summed images. Recently, diagnostic improvement in specificity has been demonstrated by “motion-frozen” technique in MPS scans of obese patients.⁵⁷ The combination of such advanced approaches dedicated to cardiac imaging and the general advances in image reconstruction, described above, could result in further gains in image quality.

CONCLUSIONS

Nuclear cardiology imaging techniques are undergoing revolutionary changes in the last few years. Novel iterative reconstruction methods, which include modeling of physical phenomena and acquisition geometry, can facilitate the acceleration of image acquisition on standard gamma cameras approximately by a factor of at least 2 or more with equivalent image quality. Novel dedicated detectors and collimators optimized specifically for MPS combined with these new reconstruction approaches achieve scan times as short as 2 minutes.

These new developments facilitate new imaging protocols with improved patient comfort, increased throughput, and reduced radiation dose.

Acknowledgments

Daniel Berman has equity position in Spectrum Dynamics, Inc. We would like to acknowledge help of the following individuals who have sent material, data, and images relating to specific technologies: Gordon DePuey, Columbia University, NYC; Gary Heller University of Connecticut School of Medicine CT; Ernest V. Garcia, Emory University, Atlanta, GA; Hans Vija, Siemens Medical Solutions, Hoffman Estates, IL; Horace Hines and Angela Da Silva Philips, Malpitas, CA; Dennis Kirch, Nuclear Research, Denver, CO; Dalia Sherry, Spectrum Dynamics (Haifa, Israel); Terri Garner (CardiArc, In, TX); Richard Conwell (Digirad, San Diego, CA); Frank Anstett (GE HealthCare).

In addition, we would like to thank Joyoni Dey, University of Massachusetts, Worcester, and Gillian Haemer, University of Southern California, LA, for comments and proofreading the text.

References

1. Slomka PJ, Berman DS, Germano G. Applications and software techniques for integrated cardiac multimodality imaging. *Expert Rev Cardiovasc Ther* 2008;6:27-41.
2. Einstein AJ, Henzlova MJ, Rajagopalan S. Estimating risk of cancer associated with radiation exposure from 64-slice computed tomography coronary angiography. *JAMA* 2007;298:317-23.
3. Babla H, Bai C, Conwell R. A triple-head solid state camera for cardiac single photon emission tomography (SPECT). In: Franks LA, Burger A, James RB, Barber HB, Doty FP, Roehrig H, editors. *Proceedings of the SPIE*. vol. 6319. 2005. p. 63190M.
4. Lewin HC, Hyun MC. A clinical comparison of an upright triple-head digital detector system to a standard supine dual-head gamma camera (abstract). *J Nucl Cardiol* 2005;12:113-113.
5. Bai C, Conwell R, Babla H, et al. Improving image quality and imaging efficiency using nSPEED. http://www.digirad.com/downloads_2007/nSPEED_white_paper.pdf. Accessed 30 May 2008.
6. Maddahi J, Mahmarian J, Mendez R, et al. Prospective multi-center evaluation of rapid gated SPECT myocardial perfusion upright imaging (abstract). *J Nucl Med* 2008;49:2P.
7. www.CardiArc.com. Accessed 30 May 2008.
8. Madsen MT. Recent advances in SPECT imaging. *J Nucl Med* 2007;48:661-73.
9. Arlt R, Rundquist DE. Room temperature semiconductor detectors for safeguards measurements. *Nucl Instrum Methods Phys Res A* 1996;380:455-61.
10. O'Connor M. Evaluation of the CardiArc dedicated cardiac system (unpublished independent evaluation). Rochester, MN: Mayo Clinic; 2005.
11. Sharir T, Ben-Haim S, Merzon K, et al. High-speed myocardial perfusion imaging Initial clinical comparison with conventional dual detector angler camera imaging. *J Am Coll Cardiol Cardiovasc Imaging* 2008;1:156-63.
12. Rouso B, Nagler M. Spectrum Dynamics LLC, assignee. Multi-dimensional image reconstruction. US patent 7176466. 13 Feb 2007.

13. Hines H, Kayayan R, Colsher J, et al. Recommendations for implementing SPECT instrumentation quality control. *Eur J Nucl Med Mol Imaging* 1999;26:527-32.
14. Patton J, Sandler M, Berman D, et al. D-SPECT: A new solid state camera for high speed molecular imaging. *Soc Nuclear Med* 2006;47:189-189.
15. Ben-Haim S, Hutton B, Van Gramberg D, et al. Simultaneous dual isotope myocardial perfusion scintigraphy (DI MPS)—Initial experience with fast D-SPECT (abstract). *J Nucl Cardiol* 2008;15:S2.
16. Berman D, SW H, Wolak A, et al. Stress thallium-201/rest Tc-99m sequential dual isotope high-speed myocardial perfusion imaging. *Circulation* 2008;118:S1010.
17. Sharir T, Ben Haim S, Slomka PJ, et al. Validation of quantitative analysis of high-speed myocardial perfusion imaging: Comparison to conventional SPECT imaging (abstract). *J Nucl Cardiol* 2008;15:S4.
18. Jaszczak RJ, Li J, Wang H, Zalutsky MR, Coleman RE. Pinhole collimation for ultra-high-resolution, small-field-of-view SPECT. *Phys Med Biol* 1994;39:425-37.
19. Schramm NU, Ebel G, Engeland U, Schurrat T, Behe M, Behr TM. High-resolution SPECT using multipinhole collimation. *IEEE Trans Nucl Sci* 2003;50:315-20.
20. Beekman FJ, Vastenhouw B. Design and simulation of a high-resolution stationary SPECT system for small animals. *Phys Med Biol* 2004;49:4579-92.
21. Funk T, Kirch DL, Koss JE, Botvinick E, Hasegawa BH. A novel approach to multipinhole SPECT for myocardial perfusion imaging. *J Nucl Med* 2006;47:595-602.
22. Metzler SD, Bowsher JE, Smith MF, Jaszczak RJ. Analytic determination of pinhole collimator sensitivity with penetration. *IEEE Trans Med Imaging* 2001;20:730-41.
23. Funk T, Després P, Barber WC, Shah KS, Hasegawa BH. A multipinhole small animal SPECT system with submillimeter spatial resolution. *Med Phys* 2006;33:1259-68.
24. Steele PP, Kirch DL, Koss JE. Comparison of simultaneous dual-isotope multipinhole SPECT with rotational SPECT in a group of patients with coronary artery disease. *J Nucl Med* 2008;49:1080.
25. Volokh L, Hugg J, Blevis I, Asma E, Jansen F, Manjeshwar R. Effect of detector energy response on image quality of myocardial perfusion SPECT. Paper presented at IEEE nuclear science symposium and medical imaging conference, 19–26, 2008; Dresden.
26. Blevis I, Tsukerman L, Volokh L, Hugg J, Jansen F, Bouhnik J. CZT gamma camera with pinhole collimator: Spectral measurements. Paper presented at IEEE 2008 nuclear science and medical imaging conference, 2008; Dreseden, Germany.
27. Garcia EV, Tsukerman L, Keidar Z. 2.05: A new solid state, ultra fast cardiac multi-detector SPECT system. *J Nucl Cardiol* 2008;15:S3-S3.
28. Hawman PC, Haines EJ. The cardiofocal collimator: A variable focus collimator for cardiac SPECT. *Phys Med Biol* 1994;39:439-50.
29. Vija A, Hawman E, Engdahl J. Analysis of a SPECT OSEM reconstruction method with 3D beam modeling and optional attenuation correction: Phantom studies. Paper presented at IEEE nuclear science symposium and medical imaging conference, 2003.
30. Römer W, Reichel N, Vija HA, et al. Isotropic reconstruction of SPECT data using OSEM3D: Correlation with CT. *Acad Radiol* 2006;13:496-502.
31. Vija H, Chapman J, Ray M. IQ•SPECT technology white paper. Siemens Medical Solutions, USA. *Mol Imaging* 2008;1-7.
32. Shepp LA, Vardi Y. Maximum likelihood reconstruction for emission tomography. *IEEE Trans Med Imaging* 1982;1:113-22.
33. Lange K, Carson R. EM reconstruction algorithms for emission and transmission tomography. *J Comput Assist Tomogr* 1984;8:306-16.
34. Hudson HM, Larkin RS. Accelerated image reconstruction using ordered subsets of projection data. *IEEE Trans Med Imaging* 1994;13:601-9.
35. El Fakhri G, Buvat I, Benali H, Todd-Pokropek A, Di Paola R. Relative impact of scatter, collimator response, attenuation, and finite spatial resolution corrections in cardiac SPECT. *J Nucl Med* 2000;41:1400-8.
36. Metz CE. The geometric transfer function component for scintillation camera collimators with straight parallel holes. *Phys Med Biol* 1980;25:1059-70.
37. Kadmas DJ, Frey EC, Karimi SS, Tsui BMW. Fast implementation of reconstruction-based scatter compensation in fully 3D SPECT image reconstruction. *Phys Med Biol* 1998;43:857-73.
38. Ye J, Song X, Zhao Z, Da Silva AJ, Wiener JS, Shao L. Iterative SPECT reconstruction using matched filtering for improved image quality. *IEEE Nucl Sci Symp Conf Rec* 2006;4.
39. Ye J, Shao L, Zhao Z, Durbin M. Iterative reconstruction with enhanced noise control filtering. WO patent WO/2007/034,342; 2007.
40. Van Laere K, Koole M, Lemahieu I, Dierckx R. Image filtering in single-photon emission computed tomography: Principles and applications. *Comput Med Imaging Graph* 2001;25:127-33.
41. Venero CV, Ahlberg AW, Bateman TM, et al. Enhancement of nuclear cardiac laboratory efficiency—Multicenter evaluation of a new post-processing method with depth-dependent collimator resolution applied to full and half-time acquisitions. *J Nucl Cardiol* 2008;15:S4.
42. Bateman TM, Heller GV, McGhie AI, et al. 2.04: Multicenter investigation comparing a highly efficient half-time stress-only attenuation correction approach against standard rest-stress Tc-99m SPECT imaging. *J Nucl Cardiol* 2008;15:S3-S3.
43. Tsui BMW, Hu HB, Gilland DR, Gullberg GT. Implementation of simultaneous attenuation and detector response correction in SPECT. *IEEE Trans Nucl Sci* 1988;35:778-83.
44. DePuey E, Gadiraju R, Clark J, Thompson L, Anstett F, Shwartz S. OSEM and wide beam reconstruction (WBR) “half-time” gated myocardial perfusion SPECT functional imaging: A comparison to “full-time” filtered back projection. *J Nucl Cardiol* 2008;15:547-63.
45. Tsui BMW, Gullberg GT. The geometric transfer-function for cone and fan beam collimators. *Phys Med Biol* 1990;35:81-93.
46. Tsui BMW, Frey EC, Zhao X, Lalush DS, Johnston RE, McCartney WH. The importance and implementation of accurate 3D compensation methods for quantitative SPECT. *Phys Med Biol* 1994;39:509-30.
47. Bruyant PP. Analytic and iterative reconstruction algorithms in SPECT. *J Nucl Med* 2002;43:1343-58.
48. Green PJ. Bayesian reconstructions from emission tomography data using a modified EM algorithm. *IEEE Trans Med Imaging* 1990;9:84-93.
49. Alenius S, Ruotsalainen U. Bayesian image reconstruction for emission tomography based on median root prior. *Eur J Nucl Med Mol Imaging* 1997;24:258-65.
50. Vija AH, Zeintl J, Chapman JT, Hawman EG, Hornegger J. Development of rapid SPECT acquisition protocol for myocardial perfusion imaging. *IEEE Nucl Sci Symp Conf Rec* 2006;3:1811-6.
51. Ficaro EP, Kritzman JN, Corbett JR. 15.34: Effect of reconstruction parameters and acquisition times on myocardial perfusion distribution in normals. *J Nucl Cardiol* 2008;15:S20-S20.
52. Zeintl J, Ding X, Vija AH, Hawman EG, Hornegger J, Kuwert T. Estimation accuracy of ejection fraction in gated cardiac SPECT/

- CT imaging using iterative reconstruction with 3D resolution recovery in rapid acquisition protocols. 2007 NSS '07 IEEE Nucl Sci Symp Conf Rec 2007;6:4491-6.
53. Ultraspect. www.UltraSPECT.com. Accessed 6 Sept 2008.
 54. Borges-Neto SPR, Shaw LK, et al. Clinical results of a novel wide beam reconstruction method for shortening scan time of Tc-99m cardiac SPECT perfusion studies. *J Nucl Cardiol* 2007;14:555-65.
 55. DePuey EG, Bommireddipalli S, Beletsky I, et al. 2.01: Quarter-time myocardial perfusion SPECT wide beam reconstruction. *J Nucl Cardiol* 2008;15:S2-S2.
 56. Slomka PJ, Nishina H, Berman DS, et al. "Motion-frozen" display and quantification of myocardial perfusion. *J Nucl Med* 2004;45:1128-34.
 57. Suzuki Y, Slomka PJ, Wolak A, et al. Motion-frozen myocardial perfusion SPECT improves detection of coronary artery disease in obese patients. *J Nucl Med* 2008;49:1075-9.